

Explicit Symplectic Methods for the Nonlinear Schrödinger Equation

Hua Guan¹, Yandong Jiao¹, Ju Liu² and Yifa Tang^{1,*}

¹ LSEC, ICMSEC, Academy of Mathematics & Systems Science, Chinese Academy of Sciences, Beijing 100190, China.

² Department of Scientific Computation and Applied Software, School of Science, Xi'an Jiaotong University, Xi'an 710049, China.

Received 18 April 2008; Accepted (in revised version) 26 November 2008

Available online 13 February 2009

Abstract. By performing a particular spatial discretization to the nonlinear Schrödinger equation (NLSE), we obtain a non-integrable Hamiltonian system which can be decomposed into three integrable parts (L-L-N splitting). We integrate each part by calculating its phase flow, and develop explicit symplectic integrators of different orders for the original Hamiltonian by composing the phase flows. A 2nd-order reversible constructed symplectic scheme is employed to simulate solitons motion and invariants behavior of the NLSE. The simulation results are compared with a 3rd-order non-symplectic implicit Runge-Kutta method, and the convergence of the formal energy of this symplectic integrator is also verified. The numerical results indicate that the explicit symplectic scheme obtained via L-L-N splitting is an effective numerical tool for solving the NLSE.

AMS subject classifications: 74S30, 65Z05, 65P10, 37M15

Key words: Explicit symplectic method, L-L-N splitting, nonlinear Schrödinger equation.

1 Introduction

The nonlinear Schrödinger equation (NLSE) has been central to a variety of areas in mathematical physics for almost four decades. It is an equation for a complex field $W(x,t)$ of the following form along with initial condition:

$$\begin{cases} iW_t + W_{xx} + a|W|^2W = 0, \\ W(x,0) = W_0(x), \end{cases} \quad (1.1)$$

*Corresponding author. *Email addresses:* guanhua@amss.ac.cn (H. Guan), jiaoyd@lsec.cc.ac.cn (Y. Jiao), liujuy@gmail.com (J. Liu), tyf@lsec.cc.ac.cn (Y. Tang)

where $x \in \mathbb{R}$ and a is a constant parameter. The initial condition $W_0(x)$ conducts the motion, for instance, some $W_0(x)$'s with $W_0(\pm\infty)=0$ induce bright solitons motion; some with $|W_0(\pm\infty)| \neq 0$ lead to dark solitons motion; and periodic $W_0(x)$'s may result in periodic motion [9,22,23]. The NLSE (1.1) has an infinite number of conserved quantities [44] such as the charge, the moment, the energy, etc. We present the first six as follows:

$$F_1 = \int_{-\infty}^{+\infty} |W|^2 dx, \quad F_2 = \int_{-\infty}^{+\infty} \left\{ W \frac{d\tilde{W}}{dx} - \tilde{W} \frac{dW}{dx} \right\} dx, \quad (1.2a)$$

$$F_3 = \int_{-\infty}^{+\infty} \left\{ 2 \left| \frac{dW}{dx} \right|^2 - a |W|^4 \right\} dx, \quad (1.2b)$$

$$F_4 = \int_{-\infty}^{+\infty} \left\{ 2 \frac{d\tilde{W}}{dx} \frac{d^2W}{dx^2} - 3a |W|^2 \tilde{W} \frac{dW}{dx} \right\} dx, \quad (1.2c)$$

$$F_5 = \int_{-\infty}^{+\infty} \left\{ 2 \left| \frac{d^2W}{dx^2} \right|^2 - 6a |W|^2 \left| \frac{dW}{dx} \right|^2 - a \left(\frac{d|W|^2}{dx} \right)^2 + a^2 |W|^6 \right\} dx, \quad (1.2d)$$

$$F_6 = \int_{-\infty}^{+\infty} \left\{ 2 \frac{d^3W}{dx^3} \frac{d^2\tilde{W}}{dx^2} - 5a \left| \frac{dW}{dx} \right|^2 \frac{d|W|^2}{dx} - 10a |W|^2 \frac{d\tilde{W}}{dx} \frac{d^2W}{dx^2} + 5a^2 |W|^4 \tilde{W} \frac{dW}{dx} \right\} dx, \quad (1.2e)$$

where \tilde{W} represents the complex conjugation of W .

The NLSE above is an envelop wave equation [36] which appears in a variety of diverse physical systems, with successful applications to nonlinear optics, plasma physics and mechanics, depicting processes such as propagation of the electromagnetic field in optical fibers [16,26], the self-focusing and collapse of Langmuir waves [43], and the behavior of deep water waves in the ocean [6,28]. In the optical context, one can easily arrive at the NLSE from the Maxwell equations with nonlinear polarization when adopting envelop wave approximation by using multiscale techniques, which governs the time evolution of the slow amplitude of the wave packets [3,36]. Many research works have been done on the study of the NLSE in both the physical and the mathematical aspects of the equation. Some recent interests have been devoted to its external potentials, e.g., applications in Bose-Einstein condensates (BECs) [4,31]. The fast theoretical and experimental developments in nonlinear optics and condensed matter physics have drawn new attentions to the NLSE. An important emerging research topic is studying the discrete NLSE model (or spatial discretization version), e.g., an integrable type of discretization of the NLSE proposed by Ablowitz and Ladik [1,2] and accordingly referred to as the Ablowitz-Ladik (A-L) model:

$$i \frac{dW_l}{dt} + \frac{W_{l+1} - 2W_l + W_{l-1}}{h^2} + \frac{a}{2} |W_l|^2 (W_{l-1} + W_{l+1}) = 0, \quad (1.3)$$

and the most direct discrete NLSE is of the form

$$i \frac{dW_l}{dt} + \frac{W_{l+1} - 2W_l + W_{l-1}}{h^2} + a |W_l|^2 W_l = 0, \quad (1.4)$$

where h is the spatial step size and $W_l(t) = W(lh, t)$, $l = \dots, -1, 0, 1, \dots$. It has been proved [40, 41] that the solutions of (1.3) and (1.4) converge to the solutions to the original continuous NLSE (1.1) when $h \rightarrow 0$.

The integrability of model (1.3) makes it a fertile starting point for developing relevant perturbation theory from this well-understood limit for the existence and stability of the solitary waves [21]. A symplectic integration scheme for that is established in [39] to compute time evolution of the soliton motion, requiring a little extra work on Darboux transformation converting the generalized Hamiltonian into a standard one in order to use symplectic integrators. However, the Hamiltonian for model (1.4) is not integrable, and hence less amendable to analysis and computations. It is usually considered difficult to solve the original NLSE or the discrete NLSE, although many numerical methods and techniques have been proposed and widely used in solving the problem with much success, see, e.g., [7, 8, 13, 17–20, 24, 25, 29, 32, 33, 39, 41, 45]. The main disadvantage of these methods is that the implementation process are usually time-consuming due to the implicitness of the schemes. In this paper, we propose an L-L-N splitting technique to decompose the original model into three integrable models and compute the phase flow of each part individually. Then compose the phase flows to build the completely explicit symplectic integrator for the original model (1.4). It should be noted that symplectic integrators take advantage over non-symplectic ones (even though implicit) in long term simulations, which preserve structure and physical conservation laws.

Hereafter we take the case of bright solitons motion with $\int_{-\infty}^{+\infty} |W|^2 dx < +\infty$ as special interest, and assume the boundary condition

$$W(-(n+1)h, t) = W((n+1)h, t) = 0$$

for convenience. Setting $W_l = p_l + iq_l$, $l = \dots, -1, 0, 1, \dots$, Eq. (1.4) can be rewritten as the following Hamiltonian system

$$\frac{dZ}{dt} = J^{-1} \nabla H(Z), \tag{1.5}$$

with Hamiltonian

$$H(Z) = H(p, q) = \frac{1}{2h^2} [p^\top B p + q^\top B q] + \frac{a}{4} \sum_{k=-n}^n [p_k^2 + q_k^2]^2, \tag{1.6}$$

where $Z = [z_1, \dots, z_{4n+2}]^\top = [p^\top, q^\top]^\top$, $p = [p_{-n}, \dots, p_n]^\top$, $q = [q_{-n}, \dots, q_n]^\top$, and ∇ stands for the gradient operator,

$$J = \begin{bmatrix} O_{2n+1} & I_{2n+1} \\ -I_{2n+1} & O_{2n+1} \end{bmatrix}, \quad B = \begin{bmatrix} -2 & 1 & & & \\ 1 & -2 & 1 & & \\ & \ddots & \ddots & \ddots & \\ & & & 1 & -2 & 1 \\ & & & & 1 & -2 \end{bmatrix} \in \mathbb{R}^{(2n+1) \times (2n+1)},$$

with O_{2n+1} and I_{2n+1} denoting the $(2n+1) \times (2n+1)$ null matrix and identity matrix respectively.

It is pointed out that for some sensitive situations of NLSE (1.1) with periodic and symmetric initial value taken near a homoclinic orbit, McLachlan [30] studied the behaviors of L-N splitting symplectic schemes, for the solutions and conservation of some integrals, up to the fifth F_5 . Moreover, Tang *et al.* [41] successfully simulated the motion of bright solitons and tested the behavior of invariants F_1 - F_4 by using some implicit symplectic methods.

This paper is organized as follows: in Section 2, we describe the L-L-N splitting of the Hamiltonian, give a 2nd-order explicit symplectic scheme and its formal energy up to $\mathcal{O}(t^6)$, and display discrete approximations of the continuous invariants of F_1 - F_6 . In Section 3, we carry out numerical experiments to test the tracking ability of the explicit symplectic scheme for solitons motion, its conservative property for the invariants of the NLSE, and the convergence of its formal energy. The numerical results are compared with those obtained by a 3rd-order non-symplectic implicit Runge-Kutta method. Some concluding remarks will be given in the final section.

2 Symplectic methods via L-L-N splitting

Scovel [35] observed that the Hamiltonian $H(p, q)$ in (1.6) can be decomposed into three parts:

$$\begin{aligned} H(p, q) &= \frac{1}{2h^2} p^\top B p + \frac{1}{2h^2} q^\top B q + \frac{a}{4} \sum_{k=-n}^n [p_k^2 + q_k^2]^2 \\ &= H^{(1)}(p, q) + H^{(2)}(p, q) + H^{(3)}(p, q), \end{aligned} \quad (2.1)$$

and each part is explicitly integrable. The solution of the Hamiltonian system (1.5) is

$$p(t) = p(0), \quad (2.2a)$$

$$q(t) = q(0) + \frac{t}{h^2} B p(0), \quad (2.2b)$$

for

$$H = H^{(1)}(p, q) = \frac{1}{2h^2} [p^\top B p];$$

and

$$p(t) = p(0) - \frac{t}{h^2} B q(0), \quad (2.3a)$$

$$q(t) = q(0), \quad (2.3b)$$

for

$$H = H^{(2)}(p, q) = \frac{1}{2h^2} [q^\top B q],$$

and

$$p_k(t) = p_k(0) \cos(ar_k^2 t) - q_k(0) \sin(ar_k^2 t), \tag{2.4a}$$

$$q_k(t) = q_k(0) \cos(ar_k^2 t) + p_k(0) \sin(ar_k^2 t), \tag{2.4b}$$

for

$$H = H^{(3)}(p, q) = \frac{a}{4} \sum_{k=-n}^n [p_k^2 + q_k^2]^2,$$

where

$$r_k^2 = p_k(0)^2 + q_k(0)^2, \quad k = -n, \dots, n.$$

Let $\phi_1^t, \phi_2^t, \phi_3^t$ denote the phase flows corresponding to Hamiltonians $H^{(1)}(p, q), H^{(2)}(p, q)$ and $H^{(3)}(p, q)$ respectively. Then for system (1.5) with Hamiltonian

$$H(p, q) = H^{(1)}(p, q) + H^{(2)}(p, q) + H^{(3)}(p, q),$$

the following methods **S1** and **S2** are 1st-order and 2nd-order explicit symplectic schemes [12, 37, 42]:

1st-order Symplectic Scheme (S1) :

$$\tilde{Z} = \Phi^t(Z) = \phi_3^t \circ \phi_2^t \circ \phi_1^t(Z), \tag{2.5}$$

2nd-order Symplectic Scheme (S2) :

$$\tilde{Z} = \Psi^t(Z) = \phi_1^{\frac{t}{2}} \circ \phi_2^{\frac{t}{2}} \circ \phi_3^t \circ \phi_2^{\frac{t}{2}} \circ \phi_1^{\frac{t}{2}}(Z). \tag{2.6}$$

Moreover, it is easy to check that Scheme **S2** is reversible, i.e.,

$$(\Psi^t)^{-1} = \Psi^{-t},$$

see [10, 15, 34] for an introduction to symplectic and reversible numerical methods for Hamiltonian dynamics.

We also apply the following 3rd-order non-symplectic R-K scheme **S3** to numerical tests for comparison.

3-order R-K scheme S3:

$$\begin{cases} \tilde{Z} = Z + \frac{t}{2}[f(K_1) + f(K_2)] \\ K_1 = Z + \frac{t}{6}[3f(K_1) - \sqrt{3}f(K_2)] \\ K_2 = Z + \frac{t}{6}[\sqrt{3}f(K_1) + 3f(K_2)]. \end{cases}$$

We calculate the formal energy of **S2** up to $\mathcal{O}(t^6)$ (see [5, 14, 38] for an introduction on calculation of formal energies of symplectic schemes):

$$\begin{aligned}
\tilde{H} &= H + \frac{t^2}{12} H_{zz}^{(1)} [J^{-1} \nabla H^{(2)}]^2 + \frac{t^2}{12} H_{zz}^{(1)} [J^{-1} \nabla H^{(3)}]^2 - \frac{t^2}{24} H_{zz}^{(2)} [J^{-1} \nabla H^{(1)}]^2 \\
&\quad + \frac{t^2}{12} H_{zz}^{(2)} [J^{-1} \nabla H^{(3)}]^2 - \frac{t^2}{24} H_{zz}^{(3)} [J^{-1} \nabla H^{(1)}]^2 - \frac{t^2}{24} H_{zz}^{(3)} [J^{-1} \nabla H^{(2)}]^2 \\
&\quad + \frac{t^2}{24} H_{zz}^{(1)} [J^{-1} \nabla H^{(1)}] [J^{-1} \nabla H^{(2)}] + \frac{t^2}{24} H_{zz}^{(1)} [J^{-1} \nabla H^{(1)}] [J^{-1} \nabla H^{(3)}] \\
&\quad + \frac{t^2}{6} H_{zz}^{(1)} [J^{-1} \nabla H^{(2)}] [J^{-1} \nabla H^{(3)}] - \frac{t^2}{12} H_{zz}^{(2)} [J^{-1} \nabla H^{(1)}] [J^{-1} \nabla H^{(2)}] \\
&\quad - \frac{t^2}{12} H_{zz}^{(2)} [J^{-1} \nabla H^{(1)}] [J^{-1} \nabla H^{(3)}] + \frac{t^2}{24} H_{zz}^{(2)} [J^{-1} \nabla H^{(2)}] [J^{-1} \nabla H^{(3)}] \\
&\quad - \frac{t^2}{12} H_{zz}^{(3)} [J^{-1} \nabla H^{(1)}] [J^{-1} \nabla H^{(2)}] - \frac{t^2}{12} H_{zz}^{(3)} [J^{-1} \nabla H^{(1)}] [J^{-1} \nabla H^{(3)}] \\
&\quad - \frac{t^2}{12} H_{zz}^{(3)} [J^{-1} \nabla H^{(2)}] [J^{-1} \nabla H^{(3)}] + \mathcal{O}(t^4) \\
&= H + \tilde{H}_2 t^2 + \tilde{H}_4 t^4 + \mathcal{O}(t^6) \\
&= H_2 + \mathcal{O}(t^4) = H_4 + \mathcal{O}(t^6), \tag{2.7}
\end{aligned}$$

where

$$H_2 = H + \tilde{H}_2 t^2, \quad H_4 = H + \tilde{H}_2 t^2 + \tilde{H}_4 t^4$$

are the 2nd-order and 4th-order approximations of \tilde{H} , respectively. We write out the expansion for \tilde{H}_4 , which contains 333 terms in [11]. We use the notation

$$A_{zz}(V_1)(V_2) = \sum_{j_1, j_2=1}^{4n+2} \frac{\partial^2 A}{\partial z_{j_1} \partial z_{j_2}} [V_1]_{(j_1)} [V_2]_{(j_2)},$$

where A is one of $H^{(i)}$, $i = 1, 2, 3$, V_r ($r = 1, 2$) is one of $J^{-1} \nabla H^{(i)}$, $i = 1, 2, 3$, z_{j_u} is the j_u -th component of $(4n+2)$ -dim vector Z , and $[V_u]_{(j_u)}$ stands for the j_u -th component of $(4n+2)$ -dim vector V_u , $u = 1, 2$.

Time evolution of H_2 and H_4 will be tested for the numerical simulations in Section 3. Utilizing centered differences

$$\begin{aligned}
W_x(lh, t) &= \frac{W_{l+1} - W_{l-1}}{2h}, \\
W_{xx}(lh, t) &= \frac{W_{l+1} - 2W_l + W_{l-1}}{h^2}, \\
W_{xxx}(lh, t) &= \frac{W_{l+2} - 2W_{l+1} + 2W_{l-1} - W_{l-2}}{2h^3},
\end{aligned}$$

the conserved quantities F_1, \dots, F_6 of the original NLSE (1.1) are approximated as follows:

$$\begin{aligned} \hat{F}_1 &= h \sum_l W_l \tilde{W}_l, \quad \hat{F}_2 = \sum_l \left\{ W_l \tilde{W}_{l+1} - W_{l+1} \tilde{W}_l \right\}, \\ \hat{F}_3 &= \frac{1}{2h} \sum_l \left\{ 2|W_l|^2 - W_{l+1} \tilde{W}_{l-1} - W_{l-1} \tilde{W}_{l+1} \right\} - ah \sum_l |W_l|^4, \\ \hat{F}_4 &= \frac{1}{h^2} \sum_l \left\{ 2W_{l+1} \tilde{W}_l - 2W_l \tilde{W}_{l+1} - W_{l+1} \tilde{W}_{l-1} + W_{l-1} \tilde{W}_{l+1} \right\} \\ &\quad - \frac{3a}{2} \sum_l |W_l|^2 \tilde{W}_l \{W_{l+1} - W_{l-1}\}, \\ \hat{F}_5 &= \frac{2}{h^3} \sum_l \left\{ 6|W_l|^2 - 4W_{l+1} \tilde{W}_l - 4W_l \tilde{W}_{l+1} + W_{l+1} \tilde{W}_{l-1} + W_{l-1} \tilde{W}_{l+1} \right\} \\ &\quad - \frac{3a}{2h} \sum_l |W_l|^2 \left\{ 2|W_{l+1}|^2 - W_{l+1} \tilde{W}_{l-1} - W_{l-1} \tilde{W}_{l+1} \right\} \\ &\quad - a2h \sum_l \left\{ |W_l|^4 - |W_{l+1}|^2 |W_{l-1}|^2 \right\} + a^2 h \sum_l |W_l|^6, \\ \hat{F}_6 &= \frac{1}{h^4} \sum_l \left\{ 5W_{l+1} \tilde{W}_l - 5W_l \tilde{W}_{l+1} - 4W_{l+1} \tilde{W}_{l-1} + 4W_{l-1} \tilde{W}_{l+1} + W_{l+2} \tilde{W}_{l-1} - W_{l-1} \tilde{W}_{l+2} \right\} \\ &\quad + \frac{5a}{8h^2} \sum_l \left\{ |W_{l+1}|^2 - |W_{l-1}|^2 \right\} \left\{ W_{l+1} \tilde{W}_{l-1} + W_{l-1} \tilde{W}_{l+1} \right\} \\ &\quad + \frac{5a}{h^2} \sum_l |W_l|^2 \left\{ 2W_l \tilde{W}_{l+1} - 2W_l \tilde{W}_{l-1} + W_{l+1} \tilde{W}_{l-1} - W_{l-1} \tilde{W}_{l+1} \right\} \\ &\quad + \frac{5a^2}{2} \sum_l |W_l|^4 \tilde{W}_l \{W_{l+1} - W_{l-1}\}. \end{aligned}$$

It can be verified that F_1, F_3, F_5 are real, so are $\hat{F}_1, \hat{F}_3, \hat{F}_5$; F_2 is pure imaginary, so is \hat{F}_2 . Thus one can write

$$\begin{aligned} \hat{F}_1 &= R_1, \quad \hat{F}_3 = R_3, \quad \hat{F}_5 = R_5, \\ \hat{F}_2 &= i \cdot I_2, \quad \hat{F}_4 = R_4 + i \cdot I_4, \quad \hat{F}_6 = R_6 + i \cdot I_6. \end{aligned}$$

Moreover, it is easy to check that R_1 is an invariant of the Hamiltonian system (1.5). The evolution of R_1, \dots, I_6 will be also tested in Section 3.

3 Numerical experiments

In this section, we present the numerical simulation results to test the tracking ability of the symplectic scheme **S2** for one-soliton, two-soliton and three-soliton motion, and its

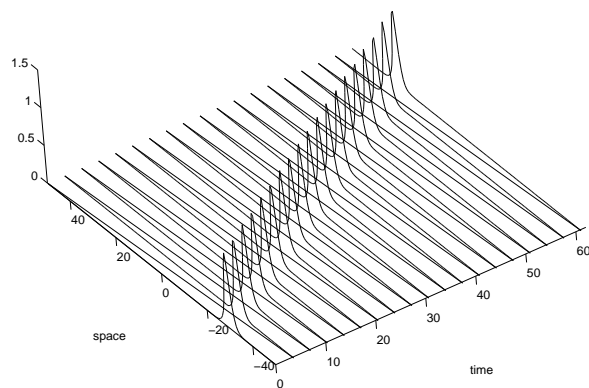


Figure 1: 1-bright-soliton evolution computed by S2.

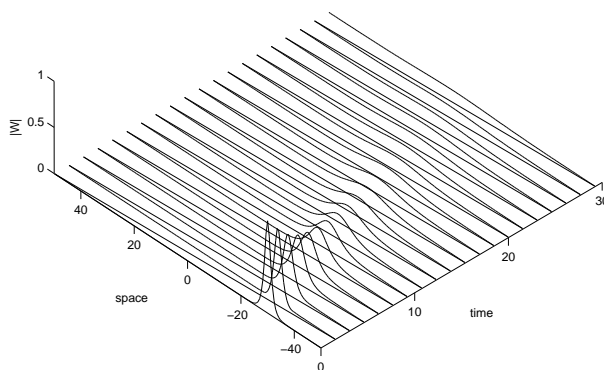


Figure 2: 1-bright-soliton evolution computed by S3.

conservative property for the discrete approximations $\hat{F}_1 - \hat{F}_6$ of the continuous invariants $F_1 - F_6$ of the NLSE, and also the convergence of its formal energy.

We define $Err(A(t)) = A(t) - A(0)$ for any variable A for this section. For the bright solitons, the following initial conditions are introduced:

B1. One-soliton solution

$$W(x,0) = 2\eta \sqrt{\frac{2}{a}} e^{2\chi x i} \operatorname{sech}[2\eta(x - x_1)]. \quad (3.1)$$

B2. Two-soliton solution

$$W(x,0) = 2\eta_1 \sqrt{\frac{2}{a}} e^{2\chi_1 x i} \operatorname{sech}[2\eta_1(x - x_a)] + 2\eta_2 \sqrt{\frac{2}{a}} e^{2\chi_2 x i} \operatorname{sech}[2\eta_2(x - x_b)]. \quad (3.2)$$

B3. Three-soliton solution

$$W(x,0) = \operatorname{sech}(x - x_3). \quad (3.3)$$

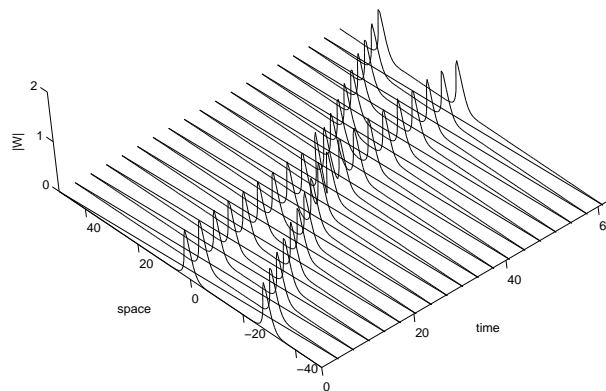


Figure 3: 2-bright-soliton evolution computed by S2.

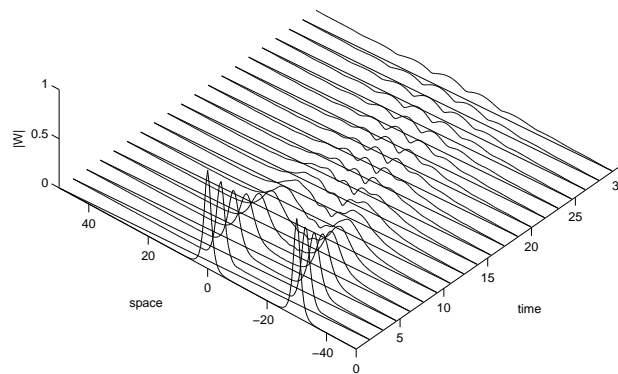


Figure 4: 2-bright-soliton evolution computed by S3.

Unless the contrary is stated the standard value for the nonlinear constant is $a = 2.0$, and the spatial step size h and temporal step sizes dt are given as follows:

$$h = 0.3 \text{ or } h = 0.15, \quad dt = 0.02 \text{ or } dt = 0.01. \tag{3.4}$$

Initial data **B1** produces the usual 1-bright-soliton solution. We present here the result of an integration with $\eta = 0.5, \chi = 0.5, x_1 = -30$ over the spatial interval $x \in [-750, 750]$ and temporal interval $t \in [0, 64]$.

The expression in **B2** is an initial data for a pair of solitons with different amplitudes and velocities, which is appropriate for the simulation of solitons collision. We have studied the following set of parameters $\eta_1 = \eta_2 = 0.5, \chi_1 = 0.25, \chi_2 = 0.025, x_a = -30, x_b = 0$ over the spatial interval $x \in [-750, 750]$ and temporal interval $t \in [0, 64]$.

From Figs. 1 and 3 with $dt = 0.02$ and $h = 0.3$, we can see that the symplectic scheme **S2** simulates the 1-bright-soliton and 2-bright-soliton motion accurately, while Figs. 2 and 4 show that the non-symplectic scheme **S3** declines clearly.

Figs. 5-8 show that in the simulation by using the scheme **S2**, the formal energy and the discrete approximations behave very well. In Fig. 5 with $h = 0.3$, one finds that the

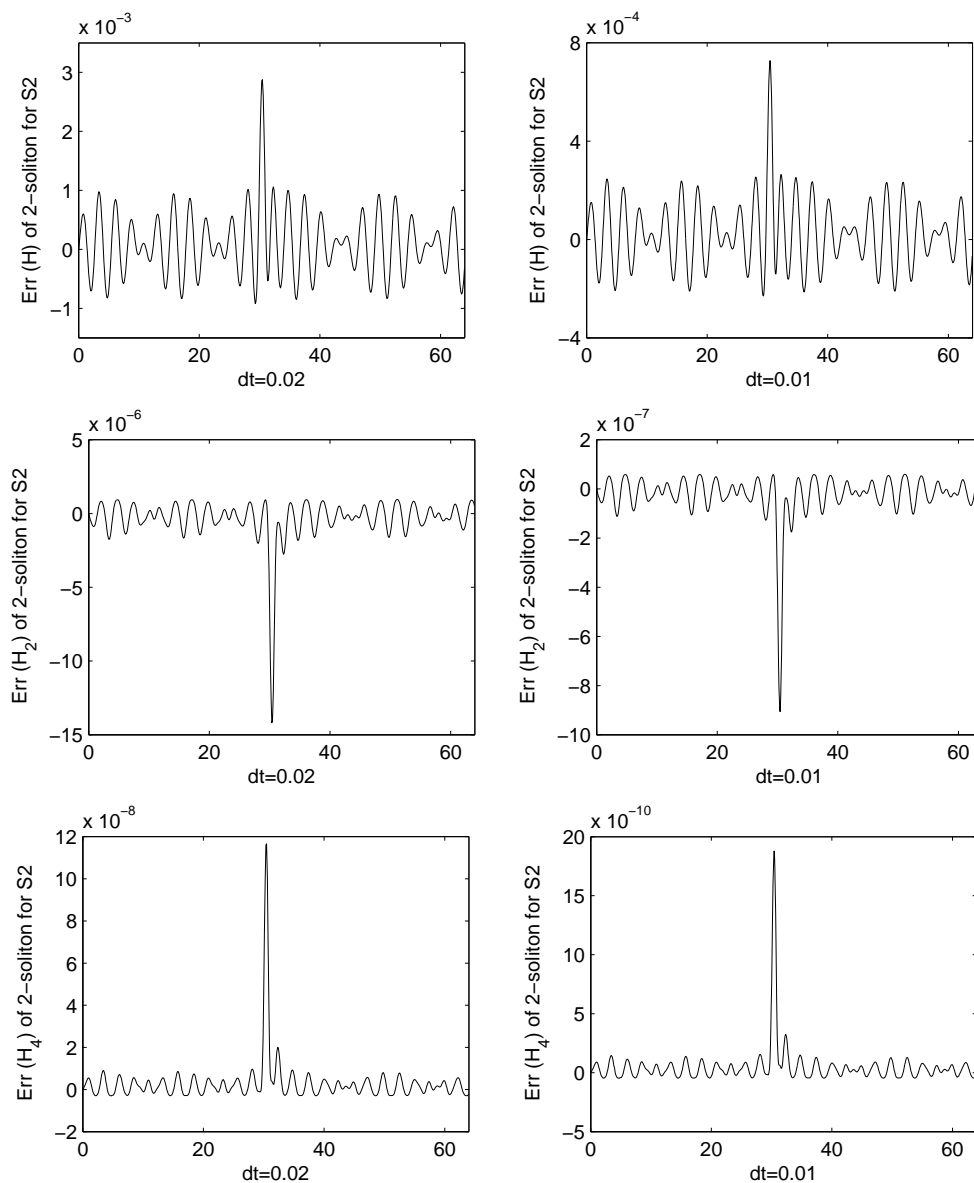


Figure 5: Evolution of formal energy obtained by S2.

amplitudes of $Err(H)$, $Err(H_2)$ and $Err(H_4)$ with $dt = 0.01$ are less than 2^{-2} , 2^{-4} and 2^{-6} times those with $dt = 0.02$ respectively.

Figs. 6-8 show the conservative property of S2, and non-conservative property of S3 for the invariants F_1 - F_6 of the NLSE (1.1). Since the evolution of other approximations is very similar, we plotted only $Err(R_1)$, $Err(I_2)$ and $Err(I_6)$ in Figs. 6-8 respectively.

Comparing the plots in the first columns of Figs. 6-8, one easily finds that like the case

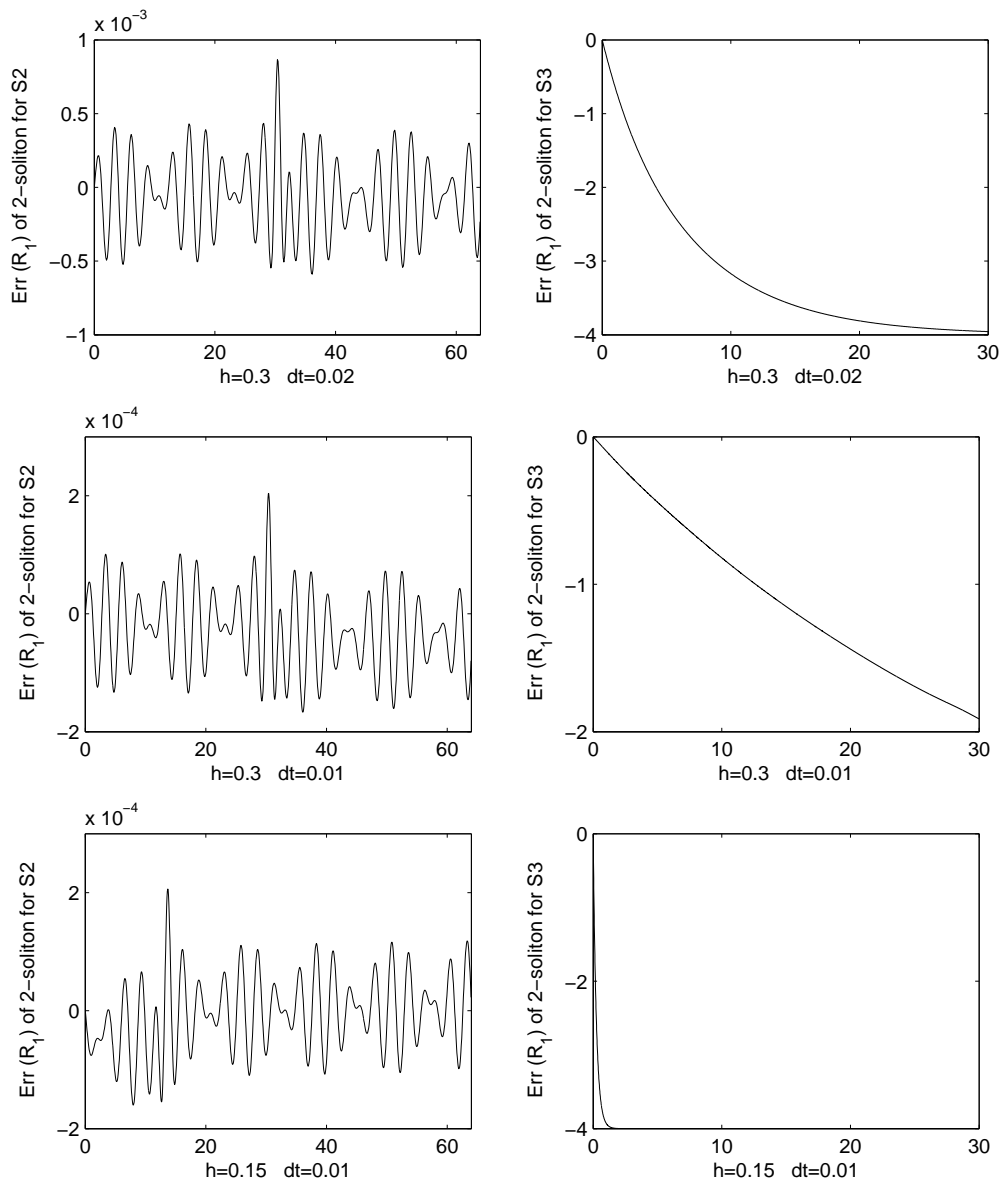


Figure 6: Evolution of R_1 obtained by S2 and S3.

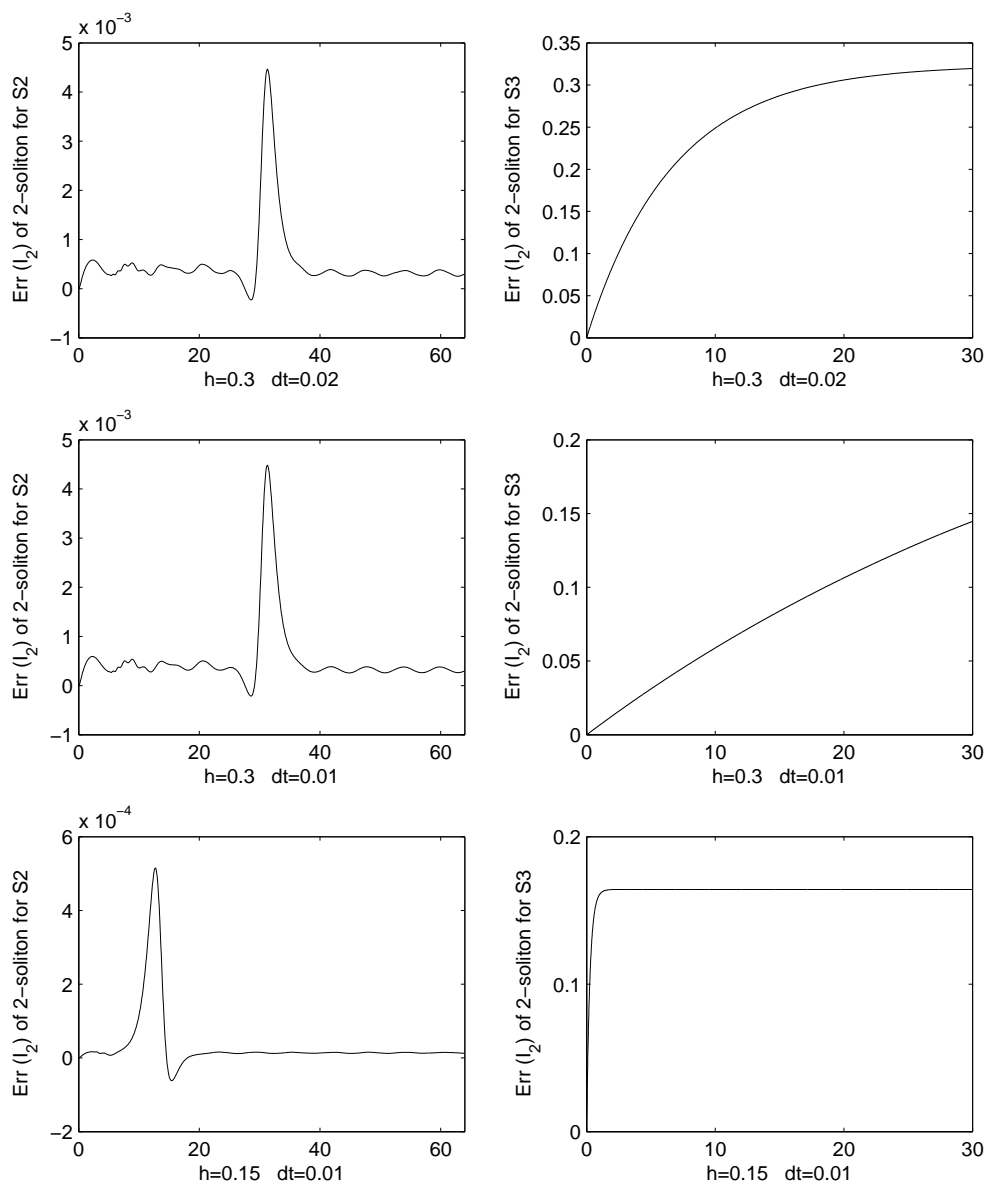
in Fig. 5,

$$Err(R_1)|_{dt=0.01} \approx 2^{-2} Err(R_1)|_{dt=0.02}.$$

Moreover,

$$Err(I_2)|_{dt=0.01} \approx Err(I_2)|_{dt=0.02}, \quad Err(I_6)|_{dt=0.01} \approx Err(I_6)|_{dt=0.02},$$

which is different from that of Fig. 5. Our explanation is that R_1 , I_2 and $R_6 + i \cdot I_6$ are

Figure 7: Evolution of I_2 obtained by S2 and S3.

approximations of the continuous invariants F_1 , F_2 and F_6 respectively, but only R_1 is still an invariant of the Hamiltonian system (1.5). $Err(I_2)$ and $Err(I_6)$ obtained by using scheme S2 depend not only on the temporal step size dt but also on the spatial step size h ; when dt is small enough, the errors depend mainly on h .

Finally, we simulate the three-soliton-bounded-state motion with initial data given by B3, which is usually considered to be a more difficult “quality” test for numerical schemes

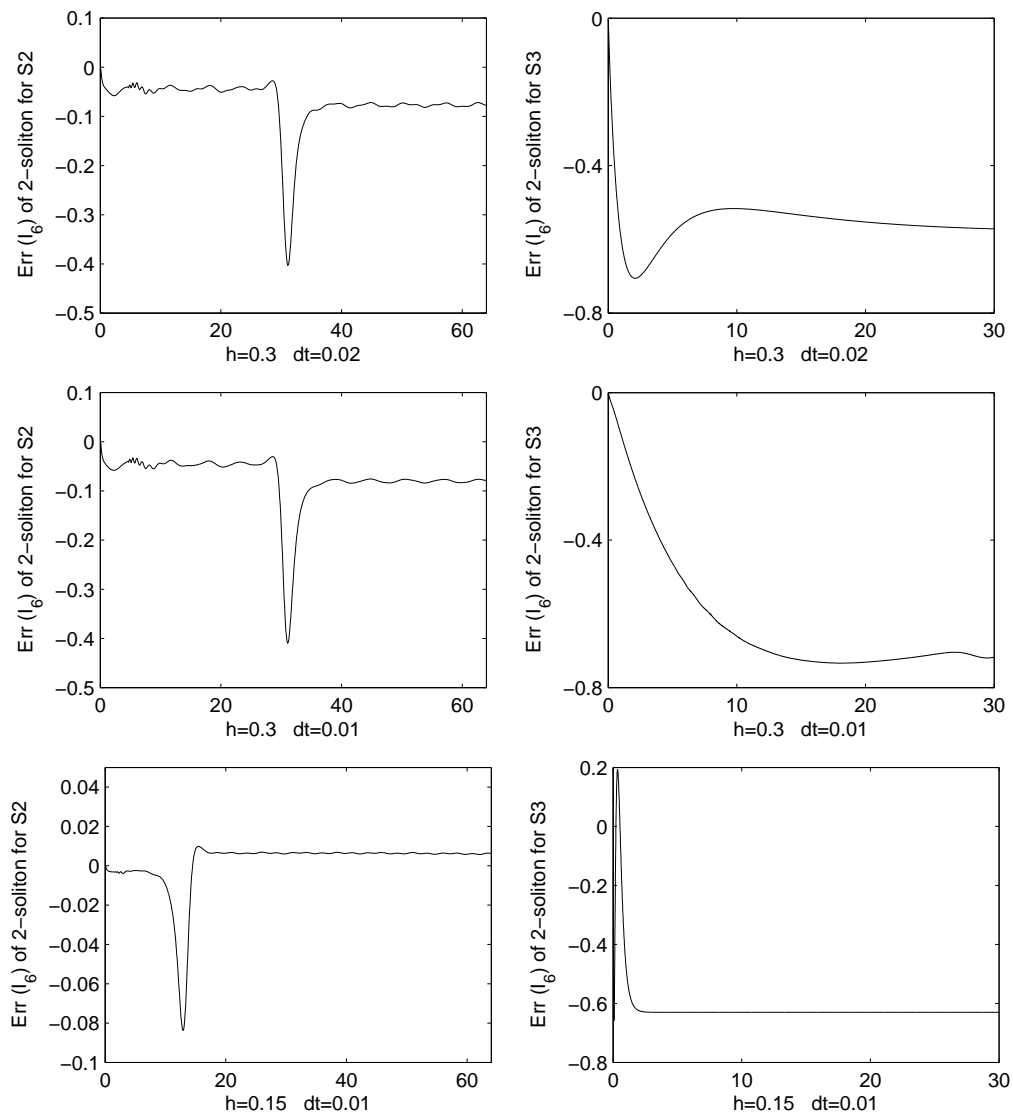


Figure 8: Evolution of I_6 obtained by S2 and S3.

because of the appearance of large spatial and temporal gradients in the solution. It has been shown that for $a = 2N^2 (N = 2, 3, \dots)$ (2.10) corresponds to a bounded state of N solitons [27]. For $a=18$ and $x_3=0.0$, we choose step sizes $h=1/15$ over the spatial interval $x \in [-20, 20]$ and temporal interval $t \in [0, 2.8]$. Fig. 9 shows that scheme S2 simulates the three-soliton motion much better than S3. To compare, we change the step size to $h=1/30$. Fig. 10 shows clearly that scheme S2 provides much more reasonable results for the three-soliton motion than those obtained by using S3.

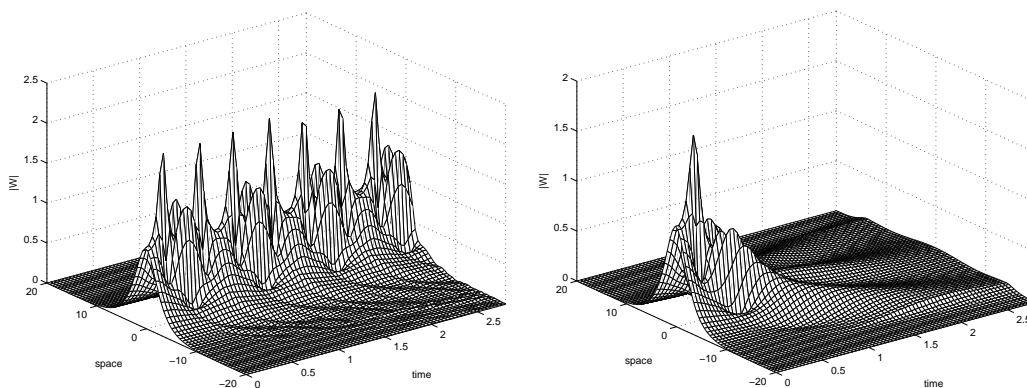


Figure 9: 3-bright-soliton evolution computed by S2 (left) and S3 (right), $h = \frac{1}{15}$.

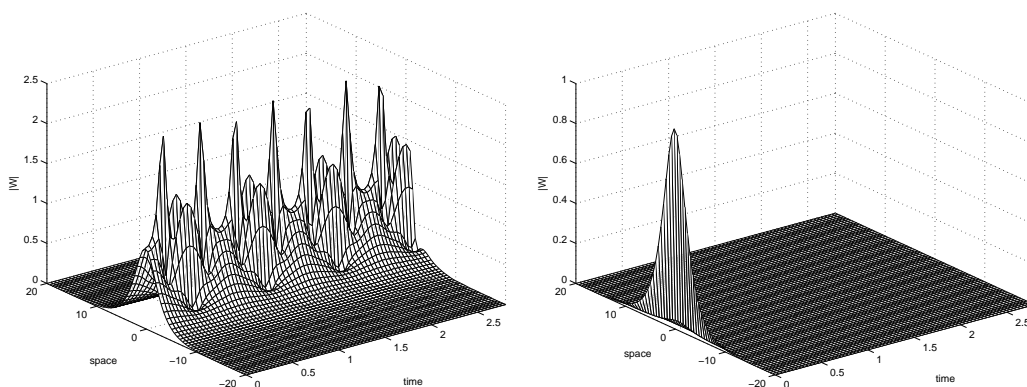


Figure 10: 3-bright-soliton evolution computed by S2 (left) and S3 (right), $h = \frac{1}{30}$.

4 Conclusions

In conclusion, we have demonstrated that via splitting technique, some completely explicit symplectic methods can be naturally applied to integrate the nonlinear Schrödinger equation. In particular, a reversible 2nd-order symplectic scheme has been used to simulate the one-soliton, two-soliton and three-soliton motion. Numerical results have shown the strong tracking ability of the scheme for solitons motion, in particular the performance of its conservative property for the invariants of the NLSE, and also the convergence of its formal energy.

Acknowledgments

We thank the referee for the valuable suggestions and comments that helped us to improve the paper. This research is partially supported by the *Informatization Construction of Knowledge Innovation* Projects of the Chinese Academy of Sciences "Supercomputing En-

vironment Construction and Application" (INF105-SCE), and by National Natural Science Foundation of China (Grant Nos. 10471145 and 10672143).

References

- [1] M.J. Ablowitz and J.F. Ladik, Nonlinear differential-difference equations, *J. Math. Phys.*, 16 (1975), 598-603.
- [2] M.J. Ablowitz and J.F. Ladik, Nonlinear differential-difference equations and Fourier analysis, *J. Math. Phys.*, 17 (1976), 1011-1018.
- [3] M.J. Ablowitz, B. Prinari and A.D. Trubatch, *Discrete and Continuous Nonlinear Schrödinger Systems*, Cambridge University Press, Cambridge, 2004.
- [4] S.K. Adhikari, Dissipation-managed soliton in a quasi-one-dimensional Bose-Einstein condensate, *Laser Phys. Lett.*, 3(11) (2006), 553-557.
- [5] G. Benettin and A. Giorgilli, On the Hamiltonian interpolation of near to the identity symplectic mappings with application to symplectic integration algorithms, *J. Stat. Phys.*, 74 (1994), 1117-1143.
- [6] T.B. Benjamin and J.E. Feir, The disintegration of wavetrains in deep water, part 1, *J. Fluid Mech.*, 27 (1967), 417-430.
- [7] J.B. Chen, M.Z. Qin and Y.F. Tang, Symplectic and multi-symplectic methods for the nonlinear Schrödinger equation, *Comput. Math. Appl.*, 43(8/9) (2002), 1095-1106.
- [8] M. Delfour, M. Fortin and G. Payre, Finite-difference solutions of a non-linear Schrödinger equation, *J. Comput. Phys.*, 44(2) (1981), 277-288.
- [9] R.K. Dodd, J.C. Eibeck, J.D. Gibbon and H.C. Morris, *Solitons and Nonlinear Wave Equation*, Academic Press, 1982.
- [10] K. Feng, *Collected Works of Feng Kang (II)*, National Defence Industry Press, Beijing, 1995.
- [11] Q.D. Feng and Y.F. Tang, Calculation of formal energies of symplectic schemes for Hamiltonian systems with applications, (2001), preprint.
- [12] E. Forest and R.D. Ruth, Fourth-order symplectic integration, *Physica D*, 43 (1990), 105-117.
- [13] B.Y. Guo, The convergence of numerical method for nonlinear Schrödinger equation, *J. Comput. Math.*, 4(2) (1986), 121-130.
- [14] E. Hairer, Backward analysis of numerical integrators and symplectic methods, *Annals Numer. Math.*, 1 (1994), 107-132.
- [15] E. Hairer, Ch. Lubich and G. Wanner, *Geometric Numerical Integration*, Springer, 2002.
- [16] A. Hasegawa, *Solitons in Optical Communications*, Clarendon Press, Oxford, 1995.
- [17] B.M. Herbst, J.L. Morris and A.R. Mitchell, Numerical experience with the nonlinear Schrödinger equation, *J. Comput. Phys.*, 60(2) (1985), 282-305.
- [18] B.M. Herbst, F. Varadi and M.J. Ablowitz, Symplectic methods for the nonlinear Schrödinger equation, *Math. Comput. Simul.*, 37 (1994), 353-369.
- [19] A.L. Islas, D.A. Karpeev and C.M. Schober, Geometric integrators for the nonlinear Schrödinger equation, *J. Comput. Phys.*, 173 (1) (2001), 116-148.
- [20] S. Jiménez, P. Pascual, C. Aguirre and L. Vázquez, A panoramic view of some perturbed nonlinear wave equations, *Inter. J. Bifur. Chaos*, 14(1) (2004), 1-40.
- [21] T. Kapitula and P. Kevrekidis, Stability of waves in discrete systems, *Nonlinearity*, 14 (2001), 533-566.
- [22] V.V. Konotop and V.E. Vekslerchik, Randomly modulated dark soliton, *J. Phys. A: Math. Gen.*, 24 (1991), 767-785.
- [23] G.L. Lamb, *Elements of Soliton Theory*, John Wiley and Sons, New York, 1980.

- [24] X.S. Liu, Y.Y. Qi and P.Z. Ding, Periodic and chaotic breathers in the nonlinear Schrodinger equation, *Chin. Phys. Lett.*, 21 (11) (2004), 2081-2084.
- [25] X.S. Liu, Y.Y. Qi, J.F. He and P.Z. Ding, Recent progress in symplectic algorithms for use in quantum systems, *Commun. Comput. Phys.*, 2 (2007), 1-53.
- [26] B.A. Malomed, Variational methods in nonlinear fiber optics and related fields, *Progress in Optics.*, 43 (2002), 69-191.
- [27] J.W. Miles, An envelope soliton problem, *SIAM J. Appl. Math.*, 41(2) (1981), 227-230.
- [28] M. Onorato, A.R. Osborne, M. Serio and S. Bertone, Freak waves in random oceanic sea states, *Phys. Rev. Lett.*, 86 (2001), 5831-5834.
- [29] V.M. Pérez-García and X.Y. Liu, Numerical methods for the simulation of trapped nonlinear Schrodinger systems, *Appl. Math. Comput.*, 144(2-3) (2003), 215-235.
- [30] R.I. McLachlan, Symplectic integration of Hamiltonian wave equation, *Numer. Math.*, 66 (1994), 465-492.
- [31] V.M. Pérez-García, H. Michinel, J.I. Cirac, M. Lewenstein and P. Zoller, Dynamics of Bose-Einstein condensates: Variational solutions of the Gross-Pitaevskii equations, *Phys. Rev. A*, 56(2) (1997), 1424-1432.
- [32] J.I. Ramos, Linearly implicit methods for the nonlinear Schrödinger equation in nonhomogeneous media, *Appl. Math. Comput.*, 133(1) (2002), 1-28.
- [33] J.M. Sanz-Serna and J.G. Verwer, Conservative and nonconservative schemes for the solution of the nonlinear Schrödinger equation, *IMA J. Numer. Anal.*, 6(1) (1986), 25-42.
- [34] J.C. Scovel, Symplectic numerical integration of Hamiltonian systems, *The Geometry of Hamiltonian Systems*, MSRI Series 22, T. Ratiu (Ed.), Springer-Verlag, New York, 1991, pp. 463-496.
- [35] J.C. Scovel and Y.F. Tang, Symplectic methods for the nonlinear Schrödinger equation, (1996), preprint.
- [36] C. Sulem and P.L. Sulem, *The Nonlinear Schrödinger Equation*, Springer-Verlag, New York, 1999.
- [37] M. Suzuki, Fractal decomposition of exponential operators with applications to many-body theories and Monte Carlo simulations, *Phys. Lett. A*, 146(6) (1990), 319-323.
- [38] Y.F. Tang, Formal energy of a symplectic scheme for Hamiltonian systems and its applications (I), *Comput. Math. Appl.*, 27(7) (1994), 31-39.
- [39] Y.F. Tang, J.W. Cao, X.T. Liu and Y.C. Sun, Symplectic methods for the Ablowitz-Ladik discrete nonlinear Schrödinger equation, *J. Phys. A: Math. Theor.*, 40(10) (2007), 2425-2437.
- [40] Y.F. Tang, V.M. Pérez-García and L. Vázquez, Symplectic methods for the Ablowitz-Ladik model, *Appl. Math. Comput.*, 82 (1997), 17-38.
- [41] Y.F. Tang, L. Vázquez, F. Zhang and V.M. Pérez-García, Symplectic methods for the nonlinear Schrödinger equation, *Comput. Math. Appl.*, 32(5) (1996), 73-83.
- [42] H. Yoshida, Construction of higher-order symplectic integrators, *Phys. Lett. A*, 150(5-7) (1990), 262-268.
- [43] V.E. Zakharov, Collapse and self-focusing of Langmuir waves, *Handbook of Plasma Physics*, 2 (1984), 81-121.
- [44] V.E. Zakharov and A.B. Shabat, Exact theory of two-dimensional self-focusing and one-dimensional self-modulation of waves in nonlinear media, *Sov. Phys. JETP*, 34(1) (1972), 62-69.
- [45] F. Zhang, V.M. Pérez-García and L. Vázquez, Numerical simulation of nonlinear Schrödinger systems: A new conservative scheme, *Appl. Math. Comput.*, 71(2-3) (1995), 165-177.